Published in final edited form as:
Clays Clay Miner. 2008 August ; 56(4): 437–452. doi:10.1346/CCMN.2008.0560405.

CHEMICAL AND MINERALOGICAL CHARACTERISTICS OF FRENCH GREEN CLAYS USED FOR HEALING

Lynda B. Williams[1], **Shelley E. Haydel**[2], **Rossman F. Giese Jr.**[3], and **Dennis D. Eberl**[4]

1 *School of Earth and Space Exploration, Arizona State University, Tempe, AZ, 85287 USA*

2 *The Biodesign Institute Center for Infectious Diseases and Vaccinology and School of Life Sciences, Arizona State University, Tempe AZ, 85287 USA*

3 *Department of Geology, 711 Natural Sciences Complex, The State University of New York, Buffalo, NY 14260 USA*

4 *U.S. Geological Survey, 3215 Marine St., Boulder, CO 80303 USA*

Abstract

The worldwide emergence of infectious diseases, together with the increasing incidence of antibiotic-resistant bacteria, elevate the need to properly detect, prevent, and effectively treat these infections. The overuse and misuse of common antibiotics in recent decades stimulates the need to identify new inhibitory agents. Therefore, natural products like clays, that display antibacterial properties, are of particular interest.

The absorptive properties of clay minerals are well documented for healing skin and gastrointestinal ailments. However, the antibacterial properties of clays have received less scientific attention. French green clays have recently been shown to heal Buruli ulcer, a necrotic or 'flesh-eating' infection caused by *Mycobacterium ulcerans*. Assessing the antibacterial properties of these clays could provide an inexpensive treatment for Buruli ulcer and other skin infections.

Antimicrobial testing of the two clays on a broad-spectrum of bacterial pathogens showed that one clay promotes bacterial growth (possibly provoking a response from the natural immune system), while another kills bacteria or significantly inhibits bacterial growth. This paper compares the mineralogy and chemical composition of the two French green clays used in the treatment of Buruli ulcer.

Mineralogically, the two clays are dominated by 1*Md* illite and Fe-smectite. Comparing the chemistry of the clay minerals and exchangeable ions, we conclude that the chemistry of the clay, and the surface properties that affect pH and oxidation state, control the chemistry of the water used to moisten the clay poultices and contribute the critical antibacterial agent(s) that ultimately debilitate the bacteria.

Keywords

illite; smectite; green clay; antibacterial; healing; mineral chemistry

*E-mail address of corresponding author: Lynda.Williams@asu.edu.

INTRODUCTION

Both animals and humans have used clay minerals for therapeutic purposes since prehistoric time (Carretero *et al.*, 2002, 2006; Wilson, 2003). In addition to the soothing effect of warm muds used in spas, cases of healing clays have also been documented (Droy-Lefaix and Tateo, 2006) primarily owing to the adsorptive property of these minerals that have extremely large relative surface areas. 'Healing clay' is a general term that includes many different mechanisms by which clays improve the health of humans (and other animals). Droy-Lefaix and Tateo (2006) reviewed studies of beneficial effects of clay minerals on gastrointestinal illnesses. The medicinal effect of clays in the gastrointestinal tract is thought to be due to adsorption of microbes, viruses, or their toxins, and modification of the mucus lining reinforcing natural defenses of the gastric tissue. Other health effects may be the supply of nutritional supplements (*e.g.* Fe, Cu) offered by some clay minerals (Aufreiter *et al.*, 1997). However, the kind of clay mineral consumed and the pH of the system are clearly important for determining whether nutrients are supplied or depleted from the body by adsorption or desorption from the clay surface (Diamond, 1999).

Some natural clay minerals have been identified that have the ability to kill a variety of pathogenic bacteria (Williams *et al.*, 2004; Ma'or *et al.*, 2006; Haydel *et al.*, 2008). This paper examines the chemical and mineralogical characteristics of two French green clays that were documented to heal Buruli ulcer, a necrotizing or 'flesh-eating' mycobacterial infection (Brunet de Courssou, 2002). One of the French green clays promoted bacterial growth, while the other substantially or completely killed bacteria. Haydel *et al.* (2008) presented a companion paper to this work, which documents the microbiological effects of the French clays on a broad spectrum of bacteria. The goal of the present paper is to compare the clays' mineralogical characteristics, major and trace element chemistry, oxidation state, pH, and surface properties that might play a role in the observed antimicrobial activity of the clays.

EVIDENCE FOR ANTIBACTERIAL CLAYS

Buruli ulcer is a chronic, necrotizing disease of the skin caused by *Mycobacterium ulcerans*. It is the third most common mycobacterial disease of immunocompetent humans with endemic rates in much of central and western Africa. In some West African communities, Buruli ulcer has replaced tuberculosis and leprosy as the most prevalent mycobacterial disease (Weir, 2002). Currently, the accepted treatment of *M. ulcerans* ulcers larger than 5 cm is surgical excision of the necrotic lesion and subsequent skin grafting. The characteristic ulcers (Figure 1) lead to very extensive skin loss; damage to nerves, blood vessels, and appendages; and overall deformity and disability. While surgery is a standard treatment for large ulcerative lesions, combined antibiotic therapy with rifampin and streptomycin reduces the extent of surgical excision and infection recurrence (WHO, 2004). However, the predilection of the disease for underprivileged populations of developing world countries makes the cost of complex surgical procedures prohibitive.

Line Brunet de Courssou, a French humanitarian working in the Ivory Coast of Africa, observed the suffering of many tribal communities where mostly women and children were afflicted with Buruli ulcer. Growing up in France, she had used a local green clay on wounds and experienced rapid healing from application of a clay paste to bug bites, stings, and cuts. She imported French clay to the Ivory Coast in an attempt to treat the skin infections of the tribal communities, and she carefully documented (photographically) the healing effects of clay on patients suffering from Buruli ulcer (Williams *et al.*, 2004). The dry French green clay was hydrated and applied as a paste directly to the ulcerated and extended healthy skin of infected patients. Throughout the course of treatment, the clay packs were removed and renewed at least once a day, with saline solution used to clean the wounds. One of the clay samples was

not as effective in killing *M. ulcerans* as the next (from a different supplier) but was more suited for promoting skin granulation after the mycobacteria were killed (Brunet de Courssou, 2002).

The clay suppliers have not revealed the geological source of the French green clays, and in fact they may be a mixture of clays from several sources (T. Ferrand, pers. comm., 2006). The primary use of these clays in France is for pelotherapy, in which a large smectite content (preferably Na-smectite) is desired for use in mineral baths or spas. The Na increases the heat capacity of montmorillonite (Ferrand and Yvon, 1991) allowing a temperature of 50°C to be sustained for treatment of rheumatism. The desirable clays are therefore from bentonites where hydrothermal activity might impose a particular chemistry on smectitic clays as they form from altered volcanic glass.

By trial and error, Brunet de Courssou developed a treatment protocol for Buruli ulcer. The stages of healing (Figure 1) show that after one day of treatment with one green clay (CsAr02), the therapeutic properties of the clay are demonstrated with the initiation of rapid, non-surgical debridement of the destroyed tissue (Figure 1b). When the edges of the skin showed signs of damage (purplish blood vessels), the second green clay (CsAg02) was administered. Extended treatment with the CsAg02 clay resulted in continued tissue regeneration and wound healing (Figure 1c,d). After several months of daily clay applications, the infection healed with soft, supple scarring and return of normal motor function (Figure 1e) (Brunet de Courssou, 2002;Williams *et al.*, 2004). Despite the observed therapeutic benefits of treating Buruli ulcer with the French clays, an approved treatment with clay depends on scientific validation of the observed effect and testing for potentially harmful side effects.

Considering the lack of therapeutics for treating this debilitating disease, the present study was undertaken to validate the observations of Brunet de Courssou by investigating the physical and chemical properties of the French clay minerals responsible for antibacterial activity. The approach is to: (1) assess the broad-spectrum antibacterial effects of the clay minerals (Haydel *et al.*, 2008); (2) examine the crystal structures and surface properties of the clay minerals; and (3) identify whether a chemical transfer (toxin or nutrient depletion) or a physical phenomenon (metal precipitate/cell suffocation) is responsible for antibacterial activity.

METHODS

Microbial susceptibility testing

Antibacterial properties of the two French green clays used in the Ivory Coast were assessed by standard microbiological protocols using bacterial strains obtained from the American Type Culture Collection (ATCC). Haydel *et al.* (2008) tested the clays against a variety of Gram-negative bacteria, Gram-positive bacteria, and mycobacteria, each with different cell membrane structure and metabolic functions. The intent was to discover if the clays killed bacterial pathogens other than the *M. ulcerans*, as a way of deducing the type of cell destruction or metabolic functions affected by the clay. In every case, the clay that inhibited growth of *E. coli* (ATCC 25922) also inhibited other pathogens tested to varying degrees; experiments on the slow-growing *M. ulcerans* are ongoing. The details of the microbiology are beyond the scope of this paper, so here reference to the microbiological results on *E. coli* alone serve as an example of the extreme responses (bactericidal activity *vs*. enhanced growth) to the French clays.

All clay mineral samples were sterilized in an autoclave (121°C, 15 psi for 1 h) before microbial testing to remove any environmental bacteria that might have adhered to mineral surfaces. The initial *E. coli* cultures were grown over 24 h and diluted with fresh Luria broth (LB) growth media to an approximate density of 5×10^7 CFU/mL (CFU: colony-forming units). To confirm

the initial bacterial counts, serially diluted bacterial cultures were plated on the appropriate agar plates and enumerated. After dilution, sterilized clay minerals (200 mg) were mixed with 400 μL of media containing the initial pathogen inoculum to achieve a consistency similar to the hydrated clay poultices used to treat Buruli ulcer patients. The bacteria-mineral mixtures were incubated on a rotating drum for 24 h at 37°C. Positive controls for growth of bacteria in the absence of clay minerals were included in each series of independent experiments. To ensure that the clay samples were sterilized after autoclaving and maintained sterilization during storage, negative control growth experiments with clay minerals in LB broth were performed throughout the course of the study. After incubation, mixtures were subjected to successive 10-fold serial dilutions in the appropriate medium, vortexed to disperse, and quantitatively cultured in duplicate onto agar plates to determine the number of viable bacteria. Additionally, 100 μL of the bacteria-clay suspension was plated directly onto agar plates to assess the bacterial viability in undiluted samples. All antimicrobial assays with specific clay minerals were performed in triplicate (Haydel *et al.*, 2008).

X-ray diffraction

The powdered clay samples from France were first analyzed by X-ray diffraction (XRD) (CuKα radiation) in bulk to quantify all mineral phases. Aliquots of the bulk samples were prepared following the procedure of Środoñ *et al.* (2001). Using a McCrone Mill, bulk clays were ground in ethanol, with 10 wt.% ZnO as an internal standard, to a nominal particle size of <20 μm, dried in a 60°C oven, sieved, and side loaded into an XRD mount to minimize orientation effects. The quantitative mineralogy was determined using a full XRD spectral-matching program, *RockJock* (Eberl, 2003). The clay-sized fraction (<2.0 μm) was separated from a new aliquot of the bulk clay by centrifugation and prepared as oriented clay mounts to determine the percentage of expandable clay minerals. The XRD patterns were recorded from air-dried and ethylene glycol vapor-treated mounts. Heat treatment (550°C for 1 h) distinguished chlorite from kaolinite-group minerals (Moore and Reynolds, 1997).

Later, separations of the 1.0–2.0 μm, 0.2–1.0 μm, and <0.2 μm fractions of the antibacterial clay were made following procedures of Jackson (1979). The XRD patterns were assessed for quantitative mineralogical differences related to the particle-size fraction.

Elemental chemistry

Bulk powders of the clay sample and <2.0 μm size separates were dissolved for analysis by inductively coupled plasma mass spectrometry (ICP-MS). The method applied (EPA method 3052) uses a 25 mL mixture of HNO_3, HF, and HCl with 100 mg of mineral sample, digested in sealed Teflon bombs by microwave heating. This method minimizes volatile loss. The ICP-MS analyses were tested using a standard (NIST SRM 2709; San Joaquin soil) to assure consistency in the results. Nonetheless, certain elements such as Si are not well ionized by ICP-MS and therefore their quantity is significantly less than reported by electron probe analysis. Fortunately most of the trace metals are well ionized and separated from isobaric interferences by choosing select isotopes. Multiple aliquots of each sample were measured at two different dilutions, and averages are reported. The ICP-MS results (μg/mL) were normalized according to the fluid:clay ratio and values are reported as ppm with respect to weight of clay (*e.g.* μg element/g clay). The relative standard deviation is <5%, except where indicated (see Results).

Leachates of the clay were prepared by sonifying 2 g of clay in 40 mL of distilled-deionized water (or multiples of these quantities), then shaking them for 24 h to equilibrate. The minerals were sedimented by centrifugation (20,000 rpm for 3 h), and the waters were analyzed by ICP-MS for soluble elements.

Measurements of pH were made on suspensions of <2.0 μm fractions of each clay in a ratio of 0.5 g clay to 10 mL of water. The samples were ultrasonified and then shaken for 24 h to hydrate and equilibrate with the fluid. Tests of the effect on pH of reducing the water content to that used in the clay poultice showed no more than a tenth log unit change. The pH was also measured on aqueous leachates of the clays.

Exchangeable ions were removed from the clay samples first using K-saturation with 1 N KCl (Jackson, 1974). For ICP-MS analysis of the exchangeable ions removed from the natural clay, ultrapure 1 N ammonium nitrate was used to avoid Cl^- interferences in the ICP-MS, thus allowing measurement of the natural K abundances.

Finally, the C and N contents of the clays were determined using an elemental analyzer (Keck Environmental Laboratory, ASU), and the S and P contents were determined by ICP-MS (at the US Geological Survey, Boulder, Colorado).

Electron microprobe

Major element abundances of the <2.0 μm fractions of the clay were analyzed using an electron microprobe. Clay suspensions were dried onto carbon tape and then coated with a thin C film for charge compensation. The beam was defocused (~10 μm) and mineral standards included enstatite (EN20), rutile (RUT54), orthoclase (ORI), wollastonite (WO81), and albite (AB127). Corrections for atomic number, absorbance, and fluorescence were made to compensate for mineral matrix effects and compositions are reported in oxide wt.%. Totals were >85%, with differences from 100% representing loss on ignition (water plus volatile elements) (Reed, 1993).

Dehydration, dehydroxylation, and oxidation

The proportion of ferric/ferrous Fe may be important to the respiration of bacteria in contact with the clay (Kostka *et al.*, 2002; Kim *et al.*, 2004). Changes in oxidation state were tested by heating the clay in aliquots exposed to 200°C, 550°C, and 900°C for 24 h each in atmosphere. The temperatures chosen for this progressive heating were based on studies showing that dehydration of Fe-rich smectites occurs by 200°C and dehydroxylation occurs by 550°C (Frost *et al.*, 2000; Heller-Kallai and Rozenson, 1980). Progressive oxidation occurs with increased temperature of heating and results in a color change from green (unheated) to grey (200°C) to orange-rust (550°C) and finally deep red-rust (900°C).

Scanning electron microscopy

In order to observe the textural effect of the clays on bacteria, critical point drying (CPD) was used to fix the bacteria before and after incubation with clay (Bennett *et al*., 2006), and then fixed bacteria were measured using scanning electron microscopy (SEM). The CPD *E. coli* were mounted on cellulose nitrate membranes and imaged using an Hitachi XL-30 SEM with large voltage (30 keV), current (2–3 nA), and 10 mm working distance. Samples were sputter coated with ~10 nm of Au to alleviate charging.

Critical point drying disrupts the contact between clays and bacteria, and therefore the clay-bacteria interface was analyzed directly using extremely low-energy imaging after incubation of the mixture for 7 h. A 5 μL *E. coli*-clay mixture was spread thinly over a 1 cm^2 area on polished graphite with no coating for charge compensation. The samples were placed in the vacuum chamber while still moist, and imaging was performed immediately using a very small voltage (1–2 keV), current (1–2 pA), and working distance (1–2 mm). These images taken using a NOVA 200 high-resolution field emission SEM, provide the best evidence of the textural relationship between the clay and bacteria.

Surface energy

In order to determine the interfacial forces between bacteria and the clay particles, the surface-tension values of both the clay particles and the bacterium in question must be measured. As an initial step, the two clay samples were examined to see if any dramatic differences exist in the surface free energy of these materials that might influence their interactions with bacteria. The free energy of a solid is determined by measuring the surface-tension components *via* traditional contact-angle measurements of liquids of known properties placed on thin oriented films of the clay deposited on clean glass slides. The contact angles are measured using a telemicroscope equipped with a goniometer scale and a single cross hair (van Oss, 1994). The contact angle, θ, is related to the surface tension components by the Young-Dupré equation:

$$\frac{1+\cos\theta}{2}\gamma_L = \sqrt{\gamma_S^{LW}\gamma_L^{LW}} + \sqrt{\gamma_S^{+}\gamma_L^{-}} + \sqrt{\gamma_S^{-}\gamma_L^{+}} \quad (1)$$

where the S refers to the solid and L to the liquid. The LW components are the Lifshitz-van der Waals interaction, the + is the Lewis acid and the − is the Lewis base functionality. The unknowns (the solid components) are determined from contact-angle measurements using at least three liquids of which two are polar. For oriented clay slides, the contact angle is measured immediately after the liquid drop is placed on the sample so as to reduce any infiltration of the liquid into the sample. Normally, smectite or smectitic clays support a drop for a sufficient time to allow this measurement (Norris, 1993).

RESULTS

Microbiology

Results of the microbiological testing with CsAg02 and CsAr02 French clays against *E. coli* (ATCC 25922) show that incubation of the bulk CsAg02 clay in suspension with the bacteria for 24 h completely kills *E. coli*, while the CsAr02 clay enhanced bacterial growth relative to the control samples, which contained no clay (Figure 2). Furthermore, clay minerals in growth media with no bacteria showed no bacterial growth (data not shown), thus verifying sterilization throughout the experiments. The clay fraction of the CsAg02 clay (the antibacterial clay) displays the same antibacterial effect as the bulk sample (Figure 2).

Mineralogy

The two French clays have a mixed mineral composition typical of most natural clay samples. Table 1 compares the abundance of minerals identified by XRD on randomly oriented bulk powders. The CsAr02 sample has more detrital impurities (quartz, calcite, K-feldspar) than the CsAg02 sample. The CsAg02 is dominated by smectite (Fe-rich), while the CsAr02 has more illite. Traces of other clay minerals (kaolinite, chlorite, phlogopite) are found as well. A second sample of the antibacterial clay was obtained from the supplier in 2005 (CsAg05). The mineralogy is shown for comparison to the first sample, to indicate the mineralogical homogeneity of this clay. Also shown is the mineralogy of the <0.2 μm fraction of the CsAg02 clay showing a reduction in detrital minerals (carbonate, feldspar, quartz, and micas). This can be seen in the XRD patterns (Figure 3) comparing different size fractions of the CsAg02 antibacterial clay.

Figure 4 compares the XRD patterns from air-dried and ethylene glycol-treated, oriented clay mounts of CsAr02 and CsAg02. The peak shift and intensity increase of the smectite 001 between 5 and 10°2θ indicates a predominance of mixed-layered illite-smectite (I-S) in the antibacterial CsAg02. The I-S is randomly ordered (smectite 001 near 5°2θ) indicating a relatively low-temperature environment of formation (<100°C; Pollastro, 1993) or a limited time at elevated temperature. The highly ordered illite and micas in both clay samples (Table 1) are formed at greater temperature and are probably detrital.

Given the mineralogical differences among the three size fractions of the CsAg02 (Figure 3), and the probability that the relative surface area influences the chemical exchange, each size fraction was tested against *E. coli*. Results of these experiments (Figure 2) indicated that the bactericidal agent is associated with the finest (<0.2 μm) fraction. The larger CsAg02 size fractions had no significant antibacterial effect on *E. coli*. Weighing the quantity of different size fractions separated from a 10 g aliquot of bulk clay (dried), a rough estimate indicates 60% of the clay sample is <0.2 μm. Size separations of the CsAr02 clay were not tested because it showed no antibacterial effect in bulk or in the <2.0 μm fraction.

Standard K-saturation of the bulk CsAg02 clay (Jackson, 1979) removed the exchangeable cations from the expandable clay, and other exchangeable ions in the sample. Incubation of *E. coli* with the K^+-exchanged CsAg02 resulted in complete loss of bactericidal activity (Figure 2). Potassium saturation of the CsAr02 clay was not done because it is not antibacterial.

Heating the CsAg02 clay to 200°C and 550°C did not change the antibacterial effect on *E. coli* (Figure 2), although after heating the clay to 900°C it was no longer bactericidal. The XRD patterns of the heated clays (Figure 5) show a decrease in the intensity of clay mineral peaks as they are progressively dehydrated and dehydroxylated. The heat treatments were not performed on CsAr02 because it is not antibacterial.

Chemical analyses

The major oxide composition (Table 2) of the two French clays (<2.0 μm fraction) shows that they are very similar in Fe content (~6 wt.% total Fe). CsAr02 is also enriched in CaO, which could be related to calcite ($CaCO_3$) identified by XRD (Table 1). However, some interlayer Ca^{2+} is likely also. The CsAg02 contains more K_2O and MgO, which are probably interlayer (K^+) and octahedral (Mg^{2+}) cations associated with the 2:1 layer clays. The major volatile anion contents are listed at the bottom of Table 2, and, in addition to water, comprise most of the LOI (analytical weight loss).

The results of the ICP-MS analyses of the two digests of French clay samples, their NH_4-exchange solutions, and aqueous leachates containing soluble elements are presented in Table 3. A comparison of the chemical variations among the different size fractions of the antibacterial CsAg02 is shown in Table 4.

Speciation

The pH and oxidation state control the speciation of elements identified by ICP-MS and, therefore, is important for evaluating the solution chemistry influenced by the clay that interacts with bacteria. The pH of CsAg02 suspension is alkaline ranging from 10.0 for the bulk powder, 9.7 in the <2.0 μm fraction, and 9.4 for the leachate (prepared for ICP-MS). The bulk powder CsAr02 pH is 8.6, the <2 μm fraction is 8.1, and the leachate is 7.8. The oxidation state of the aqueous leachate in contact with the bacteria was not determined, although the reduction potential (Jackson, 1979) of the CsAg02 clay is ~250 mV lower than CsAr02.

SEM imaging

Photomicrographs of the clay minerals (Figure 6) show different crystal shapes and sizes depending on magnification. Hexagonal plates of illite ~200 nm in diameter are shown on a sample with a 20 nm coat of Au (Figure 6a). With uncoated samples mounted on graphite, images of much smaller crystals (at 150,000×) that are rectangular (~20 nm×100 nm) or lath shaped (Figure 6b) appeared.

Images of *E. coli* before interaction with the CsAg02 clay show bacteria taken from growth media (Figure 6c), with well preserved cell-wall structures showing pili (filamentous

structures). After interaction with the CsAg02 clay, the cell walls show no pili and appear to form deeply wrinkled cavities (Figure 6d). Because the sample preparation method was identical for the images taken 'before' and 'after' clay interaction, the textural change is inferred to be a result of the interaction with clay. Sample preparations were made in triplicate in order to test for dehydration during the CPD. Each time, the bacteria looked different before and after clay incubation (as shown). Images of the clay-bacteria interface taken on uncoated samples (Figure 6e,f) show no signs of clay-mineral penetration of the bacteria or clay orientation around the cell wall.

Surface properties

The average contact angles for the two clays are shown in Table 5. The small water contact angles are indicative of high-energy solid surfaces and this is borne out by the large values for the Lewis acid parameter, γ^-. Both clays have small values for the Lewis acid parameter, γ^+. These values, along with the Lifshitz-van der Waals component, γ^{LW}, are typical of smectite or smectite-rich clays (Giese and van Oss, 2002). The surface-tension properties of both clays are very similar and indicate a strong hydrophilic (organophobic) nature for both of the French clays.

DISCUSSION

The destruction of bacterial life is dependent on the physical-chemical factors that affect the ability of a cell to grow and multiply. Antimicrobial agents either inhibit growth (bacteriostatic) or destroy cells (bactericidal). The most important factors for impeding bacterial viability are temperature, pH, osmotic pressure, oxidation state, and concentrations of nutrients and wastes (Nolte, 1982). Homeostasis (internal stability) of the cell depends on the action and interaction of a number of physiological systems, and therefore, we must consider the effect of the clay mineral surface and related aqueous solution chemistry on the functioning of the whole cell. Bactericides function by impeding nourishment, disrupting essential metabolic activities, suffocation (precipitation of a solid phase rendering the cell wall impermeable), poisoning (delivery of a toxin), or physical disruption (cell lysis by bursting or penetration) (Nolte, 1982).

Physical considerations

SEM images—Images showing the presence of lath-shaped clay crystals, in addition to hexagonal crystals in the CsAg02 sample (Figure 6b), indicate crystal growth under different temperature conditions (Lanson and Champion, 1991). Morphological and chemical differences may result from changing geological conditions over time that might impart an antibacterial chemistry or other property to one generation of crystals, but not the other. Such chemical differences (see below) among size fractions could explain why clay minerals in the coarser fractions were not antibacterial.

Images of the bacteria prepared by CPD, taken before and after interaction with the CsAg02 clay, clearly show an effect of the clay on the cell membrane (Figure 6c,d). The question is what imparts the physical damage observed in the dying *E. coli* (Figure 6d)? One possibility is that some of the heavy metals measured in the exchange solution and leachate might be precipitating on the *E. coli* cell envelope, either suffocating the bacteria or impeding efflux of wastes. *E. coli* (among other bacteria) can adsorb enough heavy metals (*e.g.* Ag, La, Cu, Cd) from 1 mM solutions to precipitate metallic crystal aggregates around the cell membrane (Mullen *et al.*, 1989). Some bacteria are nucleation sites for authigenic minerals (sulfides and clay precipitates) in metal-contaminated sediments (Ferris *et al.*, 1987). To test for precipitation of minerals, energy dispersive X-ray analyses of the cell surfaces after incubation with clay was performed. No detectable heavy metal precipitates were observed, although small peaks

were observed for Ca and P, which dominate the LB medium nutrients. The detection limits of EDS may be too high to detect lethal concentrations of metals.

Imaging by SEM of uncoated, wet suspensions of bacteria with clay (Figure 6e,f) show the remains of intact bacteria surrounded by the small clay crystals. The odd bacterial features are artifacts of dehydration in the high-vacuum chamber. These images show no orientation of the clay particles around the bacteria or penetration of the cell envelope by clay laths. This suggests that no physical attraction (adhesion) is present between the clay and the cell wall, which is consistent with the contact-angle measurements (Table 5) indicating an organophobic clay surface. Cell lysis does not appear to occur due to physical rupture by the CsAg02 clay.

Chemical considerations

Bacteria can accommodate large concentrations of toxic ions by three general mechanisms. The ions may be eliminated from the cell by efflux (Nies and Silver, 1995); the metals may complex into non-toxic molecules such as thiols (S compounds), or the metals may be buffered to an oxidation state which is within the physiological range of aerobic bacteria (Nies, 1999). Reduced metals are usually eliminated from bacterial cells by an efflux system. Therefore, the focus must be on the chemical reactants that might inhibit these protective mechanisms.

Thermal alteration—Mineralogical results by XRD indicate that the antibacterial CsAg02 clay contains more Fe-smectite than the CsAr02 clay (Table 1) and that it is destroyed through progressive heating (Figure 5). Frost *et al.* (2000) showed that Fe-rich smectites dehydrate by 200° and dehydroxylate by 550°C. This could eliminate certain volatile elements from consideration for involvement in the antibacterial mechanism. Elements that are volatile below 200°C (H, N, O, F, Cl, Br, I,) may be released during dehydration of the clay, assuming they are adsorbed species. Heating to 550°C eliminates any P, S, and Hg species associated with the hydroxyl bonds. This temperature also volatilizes organic compounds (although C is stable), indicating that the bactericide is not related to organic reactions or microbial processes. Furthermore, the oxidation of Fe that occurs upon dehydroxylation (Heller-Kallai and Rozenson, 1980) does not change the antibacterial effect.

Heating the clay to 900°C largely destroys the silicate structure of the clay minerals (Figure 5) leaving only the oxide components and the clay no longer kills *E. coli*. Elements that are volatile between 550° and 900°C include Na, K, Rb, Cs, As, Se, and Cd. Any one of these elements could be involved in the antibacterial mechanism; however some are more likely than others. Sodium and K, for example, are nutrients for bacteria and are concentrated in the LB growth medium, therefore they are not likely toxins. Rubidium is not considered a toxin; however, it may substitute for K in bacteria and potentially impact certain metabolic functions (Wackett *et al.*, 2004). The more common toxins are Cs, As, Se, and Cd, and therefore their minimum inhibitory concentrations (MIC) on *E. coli* growth must be evaluated. The elements not volatilized by heating to 900°C are heavy metals. However, these elements cannot be eliminated from consideration in the antibacterial mechanism because they are highly oxidized by heating in atmosphere. They may have played a toxic role in their more reduced states.

Size fraction—With the exception of Fe, which is slightly more abundant in the dissolved <0.2 μm fraction of CsAg02 than in the larger size fractions (Table 4), all of the other elements analyzed by ICP-MS are similar in abundance, within analytical error. The most notable attribute of the finest size fraction is the very large surface area (115.4 m^2/g), which may influence the solubility of elements involved in the antibacterial mechanism. Clearly the element(s) involved in the antibacterial mechanism are not highly soluble because multiple washings are required for separation of the <0.2 μm size fraction and it still killed *E. coli.* This implies high toxicity at low concentrations.

Iron possibly is involved in reactions that produce antibacterial agents. For example, hydroxyl radicals formed during oxidation of Fe may be destructive to cells or form products such as H_2O_2 that are destructive (Fenton, 1894; Schoonen *et al.*, 2006; Cohn *et al.*, 2006). The potential for reactions between metals and bacteria that produce superoxide radicals (*e.g.* O_2^-), must also be considered (Johnston *et al.*, 1975). While the Fe content of the two French clays is similar (Tables 2, 3), the molecular speciation and solubility may be quite different (Stucki *et al.*, 1996).

Exchangeable and soluble elements—The results showing that the CsAg02 clay no longer killed *E. coli* after cation exchange (Figure 2) suggest that either the element(s) responsible for bactericidal activity was removed by exchange or that the surface properties of the clay involved in elemental exchange were changed (*e.g.* charge satisfied), thus removing a chemical potential required for the antibacterial process. Based on these results, a chemical transfer is apparently involved. However, antibacterial activity could be the result of either delivery of a toxin or depletion of a nutrient supply needed by the cells. The surface potential of the clay might attract nutrients, *i.e.* Ca^{2+} or K^+, away from the bacteria, just as well as it might provide a toxin. Competition for nutrients in a supply-limited system is a plausible mechanism for metabolic malfunction. The clay-surface potential may control adsorption of toxic elements from the geological environment, as well as nutrients (Rogers *et al.*, 2002).

To test for chemical transfer of toxins, Metge *et al.* (2007) put the CsAg02 clay into dialysis tubing, and immersed the tubing in a culture of growing bacteria. Within a few hours, the bacteria were killed. Furthermore, *E. coli* grown to log phase, then washed and suspended in CsAg02 aqueous leachates, were completely killed within 6 h (Haydel *et al.*, 2008). These tests suggest that the leachate contains a chemical toxin or toxic reactants, rather than nutrient sequestration by the clay.

Solution chemistry

Cation exchange eliminated the antibacterial activity of CsAg02; therefore the abundance of elements in the exchange solution was evaluated. The exchange solution of the CsAg02 antibacterial clay contains elements in approximately the same abundance as the CsAr02 clay that does not kill bacteria (Table 3). Therefore, a more useful comparison is among the concentrations of elements in the aqueous leachate, which contains soluble elements transferable to the bacteria.

Compared to leachates of the CsAr02, the antibacterial CsAg02 aqueous leachate concentrates 1–2 orders of magnitude more Na, Mn, As, Ag, Mo, and U. As previously mentioned, Na is considered a nutrient at 162 mM, because the *E. coli* LB growth medium contains similar amounts (171 mM Na). Similarly, the minimum inhibitory concentration (MIC) of Mn on *E. coli* is between 50 and 600 ppm depending on the molecular species (Dendrinou-Samara *et al.*, 2002). Arsenic is present in the clay at levels that are toxic to humans (52.5 ppm) if eaten routinely. The lethal dose of arsenic ranges from 120 to 200 ppm in adults and is 2 ppm in children; however chronic ingestion of arsenic in water with concentrations above 10 ppb is considered toxic (Goldberg, 2002; Nordstrom, 2002). Arsenic is relatively soluble at pH >5.5, and over a wide range of oxidation states, so adsorption on particulates (oxides and clays) can be important for concentration in natural sediments (Goldberg, 2002; Wolthers *et al.*, 2007). While human consumption of As(III) is considered toxic, *E. coli* can adapt to As levels as high as 200 ppm using a chromosomal *ars* operon (Hedges and Baumberg, 1973; Carlin *et al.*, 1995).

The solubility of Mo (156 ppb) and U (980 ppb) in the CsAg02 clay is much greater (higher concentration) than the CsAr02 leachate (relative to total in the dissolved clay). Molybdenum (VI) in molybdate is biologically the most important heavy metal oxyanion in bacterial cells

(Nies, 1999) and is not considered toxic compared to Ag or U. Silver ions are well known antibacterial agents against a wide range of pathogenic organisms, but not all forms of Ag are antibacterial (Maple *et al.*, 1992; Feng *et al.*, 1998). The Ag^+ ion binds to proteins in the bacterial cell, including DNA and RNA, thus inhibiting replication (Hall *et al.*, 1987). The minimum inhibitory concentration of Ag^+ for *E. coli* is 1.2×10^{-3} mM (Uchida *et al.*, 2004), which is well above the concentration present in the CsAg02 solutions. Similarly, the MIC for U is ~5000 times greater than the concentrations found in the CsAg02 leachate. In fact all of the heavy metal concentrations in CsAg02 leachate that are <1 nM are below reported MIC values for *E. coli* (Weast, 1984; Nies, 1999; Dopson *et al.*, 2003). Nonetheless, the cited MICs for *E. coli* refer to concentrations of elements at pH 7 (human body average) with no specific discussion of oxidation state.

Because clay minerals may buffer an aqueous solution in contact with bacteria to conditions outside of the norm for humans, the molecular speciation of elements is important when evaluating MIC. For example, the solubility and molecular species of elements such as U are influenced by pH and oxidation state (Suzuki and Banfield, 1999; Franklin *et al.*, 2000). The toxic uranyl species (UO_2^{2+}) is highly soluble at low pH (<4) (Suzuki and Banfield, 2004) due to its high charge and attraction to carboxyl and phosphate groups on cell surfaces. Nonetheless, at elevated pH, and in reduced state (U(IV)), demonstrated for the CsAg02 clay, U is much less soluble (Suzuki and Banfield, 2004).

Further evaluation of the toxicity of all elements present in the clay leachate and their speciation as a function of pH and oxidation state is required. The activity of metals in solution may be influenced by the surface chemistry of the clays that alter their potential energy or reactivity (Stucki *et al.*, 1996). Support for this hypothesis is based on evidence that the CsAg02 leachates lose their bactericidal effect after sitting in a test tube for 6 months. Whether this is due to a change in oxidation state or another chemical effect regulated by the clay surface is unknown. The relative toxicity of elements such as Cs, Se, and Cd, indicated as potential participants in the antibacterial mechanism, depends on the action of their soluble molecular species on the cytoplasmic membrane of the bacteria (Estrela *et al.*, 1994). No one element or compound is likely to be responsible for this effect, but rather a combination, working in concert, that effectively attack the bacterial pathogens. For example, the antibacterial action of Dead Sea mud is thought to be a combination of high salinity, low pH (5.6), and high sulfide content (>1000 ppm) (Ma'or *et al.*, 2006). The mechanism by which these components kill bacteria has not yet been identified.

Aqueous molecular speciation

The pH of aqueous solutions in contact with clay is commonly controlled by the surface properties of the clay because H^+ is attracted to the negatively charged clay surface to varying degrees (Jackson, 1979). The interior pH of a cell is determined by the permeability of the cell membrane to protons, which is controlled by a number of ion-transport systems (Booth, 1985). The exterior pH (solution chemistry influenced by the clay) may or may not have an effect on the regulation of the pH in the cell interior, depending on the enzyme systems developed within the particular species. Many bacteria can adapt to varying external pH conditions; however, pH impacts the rate of chemical reactions (catalyzed by enzymes) that determines the flow of nutrients through the membrane. A drastic pH gradient across the membrane could affect many chemical systems required for bacterial viability (Mendonca *et al.*, 1994).

E. coli are neutrophiles that grow optimally between pH 6.0 and pH 8.0, but can grow more slowly at pH values somewhat beyond these limits (Kurkdjian and Guern, 1989). Therefore, *E. coli* growth may be impaired by the extreme exterior pH conditions imposed by application

of the high-pH CsAg02 paste or leachate. This alone would produce inhibitory growth conditions for *E. coli*, but not necessarily cause bactericidal activity (as observed). Nonetheless, a great abundance of hydroxyl groups has been identified as an antibacterial mechanism for some bacteria (Kodukula *et al.*, 1988). Hydroxyl anions can remove H^+ from fatty acids in the cell membrane, which affects permeability and transfer of ions in and out of the cell. Further testing of CsAg02 is needed, using alkalophiles unaffected by the high-pH clay, to determine the importance of pH. However, pH alone does not appear to be the antibacterial mechanism of the CsAg02 clay because other clays with a high pH (>9) have been tested on *E. coli* (data not shown) with no bactericidal effect. More likely, the pH and oxidation state are important in controlling the molecular species of toxic elements derived from antibacterial clay and their inhibitory concentrations.

CONCLUSION

Understanding the healing effect of French green clay on patients suffering from necrotizing Buruli ulcer is complicated by the disparate effect that the two clays had on laboratory-grown bacterial pathogens. The clay that was observed and described by Brunet de Courrsou (2002) to eliminate the *M. ulcerans* infection in human patients (CsAr02) was actually found to promote growth of *E. coli* (Figure 3) and other bacteria tested (Haydel *et al*., 2008). CsAr02 may have promoted growth of a natural consortium of bacteria potentially present in the open wounds and provoked the natural immune system of the patients to attack the *M. ulcerans* infected tissue. The presence of the immunosuppresent mycolactone toxin (George *et al.*, 2002;van der Werf *et al.*, 2003), generated by *M. ulcerans*, probably prohibited an immune system response prior to application of CsAr02. Alternatively, the absorbent smectite component of the CsAr02 clay could bind the mycolactone toxin and allow for it to be removed during daily clay poultice changes, thus potentiating an immune response.

If bacterial growth was promoted by the initial CsAr02 clay treatment, switching to the CsAg02 clay fortuitously sterilized the wounds by its demonstrated antibacterial action. This antibacterial activity allowed for and possibly aided natural skin granulation and eventual wound healing. The mechanism of this antibacterial action is still under investigation. However, the present study revealed that the clay is not physically penetrating the bacterial cells. Experimental results suggest that the chemistry of the water in contact with the clay is involved in creating a chemical condition detrimental to the growth of pathogenic bacteria. The large surface area of the clay buffers the water pH and oxidation state, controlling the solubility and molecular speciation of potential toxins derived from the clay. The antibacterial clays act like a self-contained chemical lab. Without the clay to buffer the aqueous chemistry, the antibacterial process would probably breakdown.

Acknowledgements

This research was supported by Public Health Service grant AT003618 from the National Institutes of Health, National Center for Complementary and Alternative Medicine, an ASU research initiative grant to S.E.H., and travel funds from ASU's Office of the Vice President for Research and College of Liberal Arts and Sciences. Technical support was provided by Amanda Turner (XRD), Panjai Prapaipong (ICP-MS), Lawrence Garvie (SEM), and Christine Remenih (microbiology) at ASU. Dave Metge, Ron Harvey, and Alex Blum assisted with analyses performed at the USGS (Boulder, Colorado). The authors sincerely thank Dr Thierry Ferrand and Guy Albresche in France for supplying the clay samples. Thierry Brunet de Courssou is responsible for alerting the authors to the humanitarian efforts and clinical observations of his mother, Line Brunet de Courssou, who passed away in 2006. We appreciate her hard work and careful observations documenting the effect of clay minerals on Buruli ulcer patients in western Africa.

References

Aufreiter S, Hancock RGV, Mahaney WC, Stambolic-Robb A, Sanmugadas K. Geochemistry and mineralogy of soils eaten by humans. International Journal of Food Science and Nutrition 1997;48:293–305.

Bennett, PC.; Engel, AS.; Roberts, JA. Counting and imaging bacteria on mineral surfaces: Pp. 37–78. In: Maurice, PA.; Warren, LA., editors. Methods of Investigating Microbial-Mineral Interactions, CMS Workshop Lectures. 14. The Clay Minerals Society; Chantilly, Virginia: 2006.

Booth IR. Regulation of cytoplasmic pH in bacteria. Microbiology Reviews 1985;49:359–378.

Brunet de Courssou, L. 5th WHO Advisory Group Meeting on Buruli Ulcer. Study Group Report on Buruli Ulcer Treatment with Clay; Geneva, Switzerland. 2002.

Carlin A, Shi W, Dey S, Rosen BP. The *ars* operon of *Escherichia coli* confers arsenical and antimonial resistance. Journal of Bacteriology 1995;177:981–986. [PubMed: 7860609]

Carretero MI. Clay minerals and their beneficial effects upon human health. A review. Applied Clay Science 2002;21:155–163.

Carretaro, MI.; Gomes, CSF.; Tateo, F. Clays and human health. In: Bergaya, F.; Theng, BKG.; Lagaly, G., editors. Handbook of Clay Science, Developments in Clay Science. 1. Elsevier Ltd; Amsterdam: 2006. p. 717-741.

Cohn, CA.; Mueller, S.; Wimmer, E.; Leifer, N.; Greenbaum, S.; Strongin, DE.; Schoonen, MAA. Pyrite-induced hydroxyl radical formation and its effect on nucleic acids; Geochemical Transactions. 2006. p. 11Open Access: www.geochemicaltransactions.com

Dendrinou-Samara C, Alevizoupoulou L, Iordanidis L, Samaras E, Kessissoglou DP. 15-MC-5 manganese metallacrowns hosting herbicide complexes. Structure and bioactivity. Journal of Inorganic Biochemistry 2002;89:89–96. [PubMed: 11931968]

Diamond JM. Dirty eating for healthy living. Nature 1999;400:120–121. [PubMed: 10408435]

Dopson M, Baker-Austin C, Koppineedi PR, Bond PL. Growth in sulfidic mineral environments: metal resistance mechanisms in acidophilic micro-organisms. Microbiology 2003;1490:1959–1970. [PubMed: 12904536]

Droy-Lefaix, MT.; Tateo, F. Clays and clay minerals as drugs. In: Bergaya, F.; Theng, BKG.; Lagaly, G., editors. Handbook of Clay Science, Developments in Clay Science. 1. Elsevier; Amsterdam: 2006. p. 743-753.

Eberl, DD. Users guide to RockJock: A program for determining quantitative mineralogy from powder X-ray diffraction data. 2003. USGS Open file Report 03-78. USGS

Estrela C, Sydney GB, Bammann LL, Felippe O Jr. Mechanism of action of calcium and hydroxyl ions of calcium hydroxide on tissue and bacteria. Brazilian Dental Journal 1994;6:85–90. [PubMed: 8688662]

Feng QL, Kim TN, Wu J, Park ES, Kim JO, Lim DY, Cui FZ. Antibacterial effects of Ag-HAp thin films on alumina substrates. Thin Solid Films 1998;335:214–219.

Fenton HJH. Oxidation of tartaric acid in the presence or iron. Journal of the Chemical Society 1894;65:899–910.

Ferrand T, Yvon J. Thermal properties of clay pastes for pelotherapy. Applied Clay Science 1991;6:21–38.

Ferris FG, Fyfe WS, Beveridge TJ. Bacteria as nucleation sites for authigenic minerals in a metal-contaminated lake sediment. Chemical Geology 1987;63:225–232.

Franklin NM, Stauber JL, Markich SJ, Lim RP. pH-dependent toxicity of copper and uranium to a tropical freshwater alga *(Chlorella sp.)*. Aquatic Toxicology 2000;48:275–289. [PubMed: 10686332]

Frost RL, Ruan H, Kloprogge JT, Gates WP. Dehydration and dehydroxylation of nontronites and ferruginous smectite. Thermochimica Acta 2000;346:63–72.

George KM, Chatterjee D, Gunawardana G, Welty D, Hayman J, Lee R, Small PL. Mycolactone: a polyketide toxin from *Mycobacterium ulcerans* required for virulence. Science 2002;283:854–857. [PubMed: 9933171]

Giese, RF.; van Oss, CJ. Colloid and Surface Properties of Clays and Related Minerals. Marcel Dekker; New York: 2002.

Goldberg S. Competitive adsorption of arsenate and arsenite on oxides and clay minerals. Soil Science Society of America Journal 2002;66:413–421.

Hall RE, Bender G, Marquis RE. Inhibitory and cidal antimicrobial actions of electrically generated silver ions. Journal of Oral Maxillofacial Surgery 1987;45:779–784. [PubMed: 3305838]

Haydel SE, Remineh CM, Williams LB. Broad-spectrum in vitro antibacterial activities of clay minerals against antibiotic-susceptible and antibiotic-resistant bacterial pathogens. Journal of Antimicrobial Chemotherapy. 2008in press

Hedges RW, Baumberg S. Resistance to arsenic compounds conferred by a plasmid transmissible between strains of *Escherichia coli*. Journal of Bacteriology 1973;115:459–460. [PubMed: 4577750]

Heller-Kallai L, Rozenson I. Dehydroxylation of dioctahedral phyllosilicates. Clays and Clay Minerals 1980;28:355–368.

Jackson, ML. Soil Chemical Analysis–Advanced course. 2. Published by the author; Madison, Wisconsin 53705, USA: 1979.

Johnston RB, Keele BB, Misra HP, Leymeyer JE, Webb LS, Baehner RL, Rajagopalan KV. The role of superoxide anion generation in phagocytic bactericidal activity. The Journal of Clinical Investigation 1975;55:1357–1372. [PubMed: 166094]

Kim J, Dong H, Seabaugh J, Newell SW, Eberl DD. Role of microbes in the smectite to illite reaction. Science 2004;303:830–832. [PubMed: 14764877]

Kodukula, PS.; Prakasam, TBS.; Antonisen, AC. Role of pH in biological wastewater treatment process. In: Bazin, MJ.; Prosser, JI., editors. Physiological Models in Microbiology. 1. CRC Press; Boca Raton, Florida: 1988. p. 114-134.

Kostka JE, Dalton DD, Skelton H, Dollhopf S, Stucki JW. Growth of iron (III)-reducing bacteria on clay minerals as the sole electron acceptor and comparison of growth yields on a variety of oxidized iron forms. Applied and Environmental Microbiology 2002;68:6256–6262. [PubMed: 12450850]

Kurkdjian A, Guern J. Intracellular pH: Measurement and importance in cell activity. Annual Reviews Plant Physiology Plant Molecular Biology 1989;40:271–303.

Lanson B, Champion D. The I-S to illite reaction in the late stages of diagenesis. American Journal of Science 1991;291:473–506.

Ma'or Z, Henis Y, Along Y, Orlov E, Sorensen KB, Oren A. Antimicrobial properties of Dead Sea black mineral mud. International Journal of Dermatology 2006;45:504–511. [PubMed: 16700781]

Maple PA, Hamilton-Miller JM, Brumfitt W. Comparison of the in-vitro activities of the topical antimicrobials azelaic acid, nitrofurazone, silver sulphadiazine and mupirocin against methicillin-resistant Staphylococcus aureus. Journal of Antimicrobial Chemotherapy 1992;29:661–668. [PubMed: 1506349]

Mendonca AF, Amoroso TL, Knabel SJ. Destruction of gram-negative food-borne pathogens by high pH involves disruption of the cytoplasmic membrane. Applied and Environmental Microbiology 1994;60:4009–4014. [PubMed: 7993089]

Metge, D.; Harvey, R.; Eberl, D.; Williams, LB. Geological Society of America. Abstracts with Programs; Denver, Colorado: 2007. Bactericidal properties of clays used for treatment of Buruli ulcer – an emerging public health threat.

Moore, DM.; Reynolds, RC. X-ray Diffraction and the Identification and Analysis of Clay Minerals. 2. Oxford University Press; New York: 1997.

Mullen MD, Wolf DC, Ferris FG, Beveridge TJ, Flemming CA, Bailey GW. Bacterial sorption of heavy metals. Applied and Environmental Microbiology 1989;55:3143–3149. [PubMed: 2515800]

Nies DH. Microbial heavy-metal resistance. Applied Microbiology Biotechnology 1999;51:730–750.

Nies DH, Silver S. Ion efflux systems involved in bacterial metal resistances. Journal of Industrial Microbiology 1995;14:186–199. [PubMed: 7766211]

Nolte, WA. Oral Microbiology. 4. Mosby; London: 1982. p. 3-37.

Nordstrom DK. Worldwide occurrences of arsenic in groundwater. Science 2002;296:2143–2145. [PubMed: 12077387]

Norris, J. Surface free energy of smectite clay minerals. Dissertation, SUNY; Buffalo, New York: 1993. p. 197

Pollastro RM. Considerations and applications of the illite-smectite geothermometer in hydrocarbon-bearing rocks of Miocene to Mississippian age. Clays and Clay Minerals 1993;41:119–133.

Reed, SJB. Electron Microprobe Analysis. 2. Cambridge University Press; Cambridge, UK: 1993. p. 326

Rogers JR, Bennett PC. Microbial release and utilization of inorganic nutrients from feldspar, basalt, and glass. Chemical Geology 2004;203:91–108.

Schoonen, MAA.; Cohn, CA.; Roemer, E.; Laffers, R.; Simon, SR.; O'Riordan, T. Mineral-induced formation of reactive oxygen species. In: Sahai, N.; Schoonen, MAA., editors. Medical Mineralogy and Geochemistry, Reviews in Mineralogy and Geochemistry. 64. Mineralogical Society of America; Chantilly, Virginia: Geochemical Society; Washington, D.C: 2006. p. 179-221.

Środoñ J, Drits VA, McCarty DK, Hsieh JC, Eberl DD. Quantitative X-ray diffraction analysis of clay bearing rocks from random preparations. Clays and Clay Minerals 2001;49:514–528.

Stucki JW, Bailey GW, Gan H. Oxidation-reduction mechanisms in iron-bearing phyllosilicates. Applied Clay Science 1996;10:417–430.

Suzuki, Y.; Banfield, JF. Geomicrobiology of Uranium. In: Burns, PC.; Finch, R., editors. Uranium: Mineralogy, Geochemistry and the Environment, Reviews in Mineralogy. 38. Mineralogical Society of America; Washington, D.C: 1999. p. 393-432.

Suzuki Y, Banfield JF. Resistance to and accumulation of uranium by bacteria from a uranium-contaminated site. Geomicrobiology Journal 2004;21:113–121.

Uchida M, Yamamoto T, Furuhashi H, Nakata S, Nakagawa Z. Antibacterial activity of silver ions at a minimum inhibitory concentration. Journal of Antibacterial and Antifungal Agents 2004;32:115–121.

van der Werf TS, Stinear T, Stienstra Y, van der Graaf WT, Small PL. Mycolactones and *Mycobacterium ulcerans* disease. Lancet 2003;362:1062–1064. [PubMed: 14522538]

van, Oss CJ. Interfacial Forces in Aqueous Media. Marcel Dekker; New York: 1994. p. 440

Wackett LP, Dodge AG, Ellis LB. Microbial genomics and the periodic table. Applied and Environmental Microbiology 2004;70:647–655. [PubMed: 14766537]

Weast, RC. Handbook of Chemistry and Physics. 64. CRC; Boca Raton, Florida: 1984.

Weir E. Buruli ulcer: the third most common mycobacterial infection. Canadian Medical Association Journal 2002;166:1691. [PubMed: 12126327]

Williams LB, Holland M, Eberl DD, Brunet T, Brunet de Courssou L. Killer Clays! Natural antibacterial clay minerals. Mineralogical Society Bulletin 2004;139:3–8.

Wilson MJ. Clay mineralogical and related characteristics of geophagic materials. Journal of Chemical Ecology 2003;29:1525–1547. [PubMed: 12921434]

Wolthers M, Butler IB, Rickard D. Influence of arsenic on iron sulfide transformations. Chemical Geology 2007;236:217–227.

World Health Organization. Provisional guidance on the role of specific antibiotics in the management of *Mycobacterium ulcerans* disease (Buruli ulcer). World Health Organization; Geneva, Switzerland: 2004.

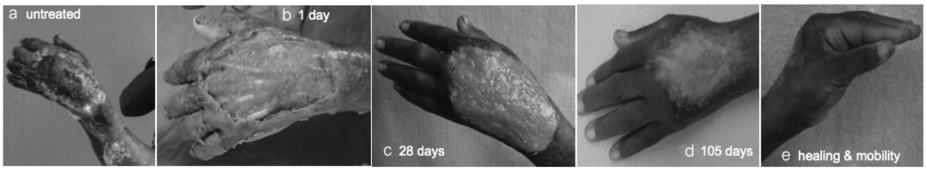

Figure 1.

A photographic example of the stages of healing by clay: destroyed tissue (a) is easily removed by one treatment with CsAr02 to expose raw muscle and bone (b). The progression of healing is shown (c, d) with daily treatments of CsAg02. After 3–4 months, the infection is healed with soft, supple scarring and a return of normal motor function (e).

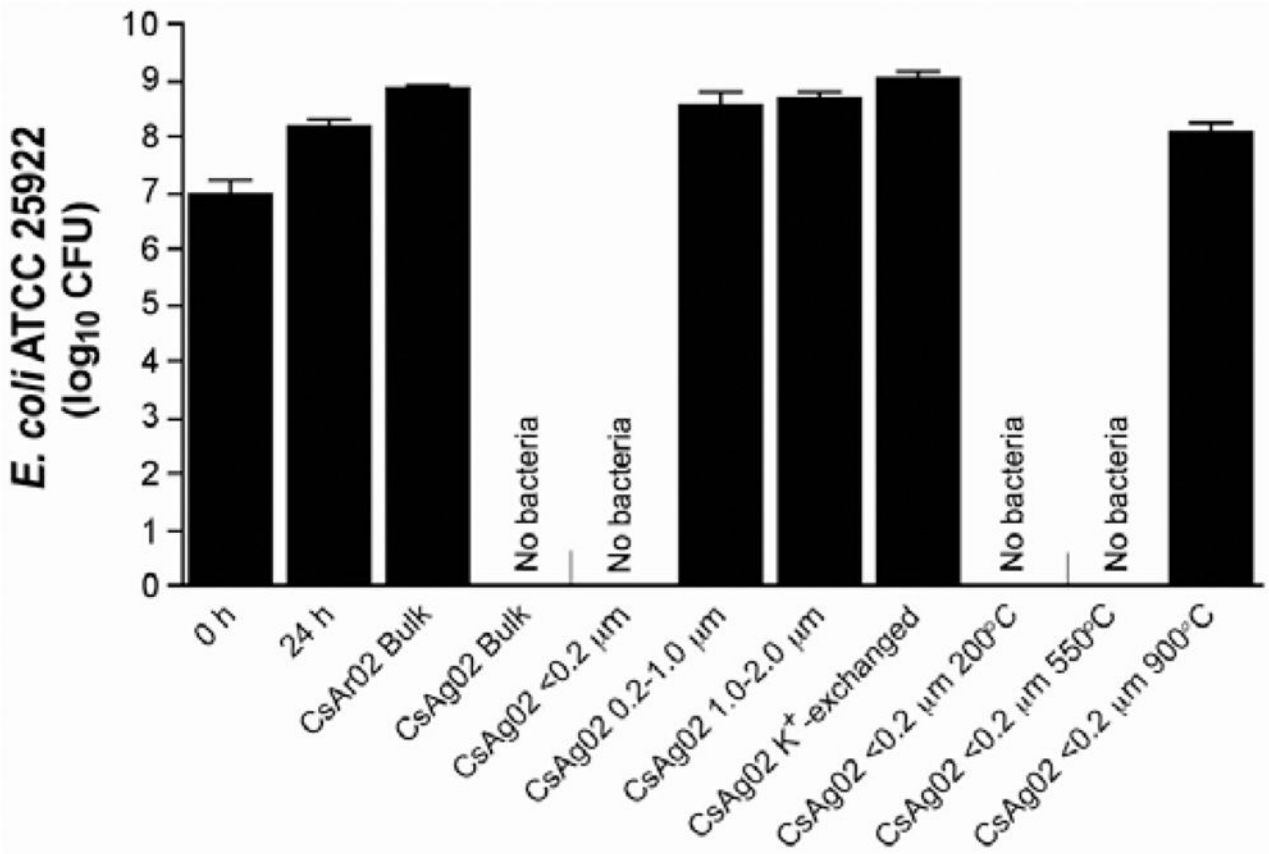

Figure 2.

Effects of CsAr02 bulk clay compared to the CsAg02 French clay on the growth of *E. coli* after size separation, exchange, and heating (see text). All *E. coli* susceptibility experiments with clay samples were incubated for 24 h at 37°C. The first two bars represent the initial *E. coli* concentration before the addition of clay and *E. coli* growth in media for 24 h at 37°C, respectively. The reported values represent the average and standard deviation of at least three independent experiments.

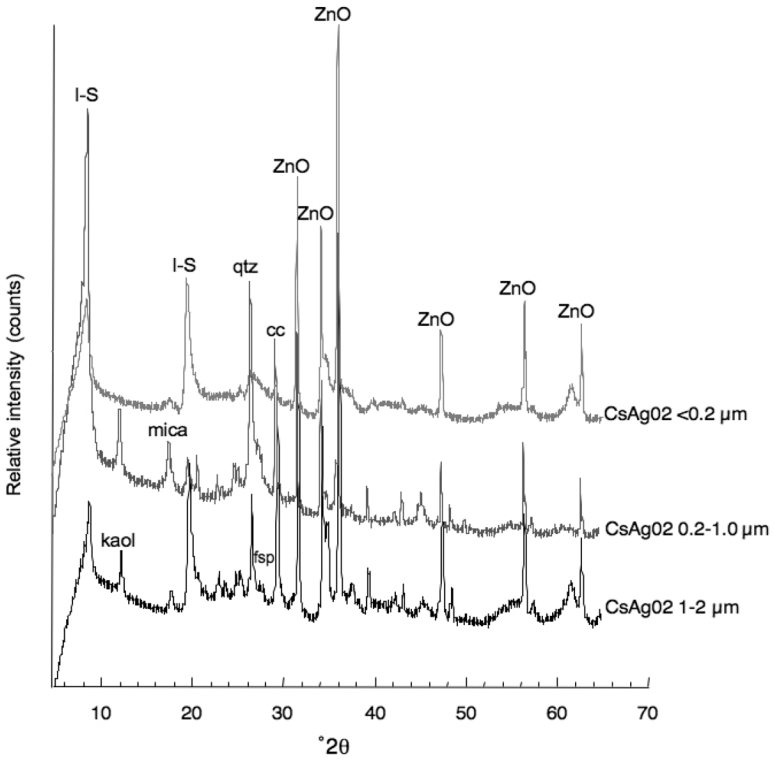

Figure 3.
Random powder XRD patterns (CuKα radiation) of different size fractions of the antibacterial CsAg02 clay, showing more detrital minerals in the coarser fractions, *e.g.* quartz (qtz), feldspar (fsp), calcite (cc), kaolinite (kaol).

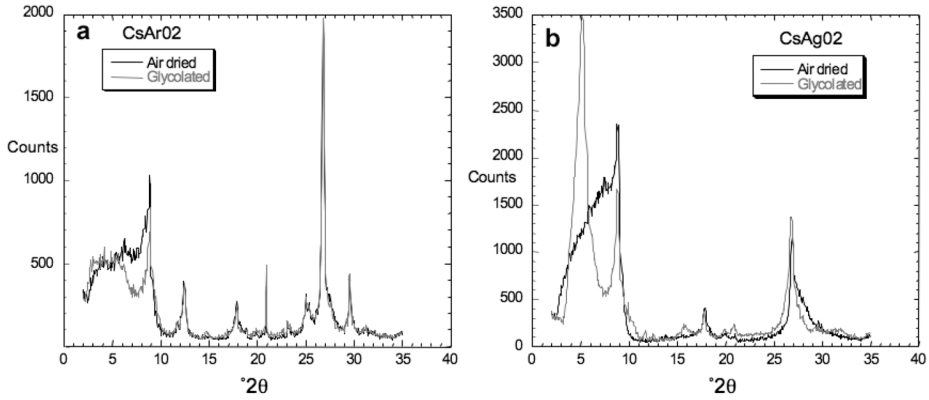

Figure 4.

Oriented clay mount XRD patterns (CuKα radiation) of <2.0 μm clay fractions of the (a) CsAr02 and (b) CsAg02 clays. Comparison of the air-dried to ethylene glycol vapor-treated preparations indicates the abundance of expandable clay (smectite).

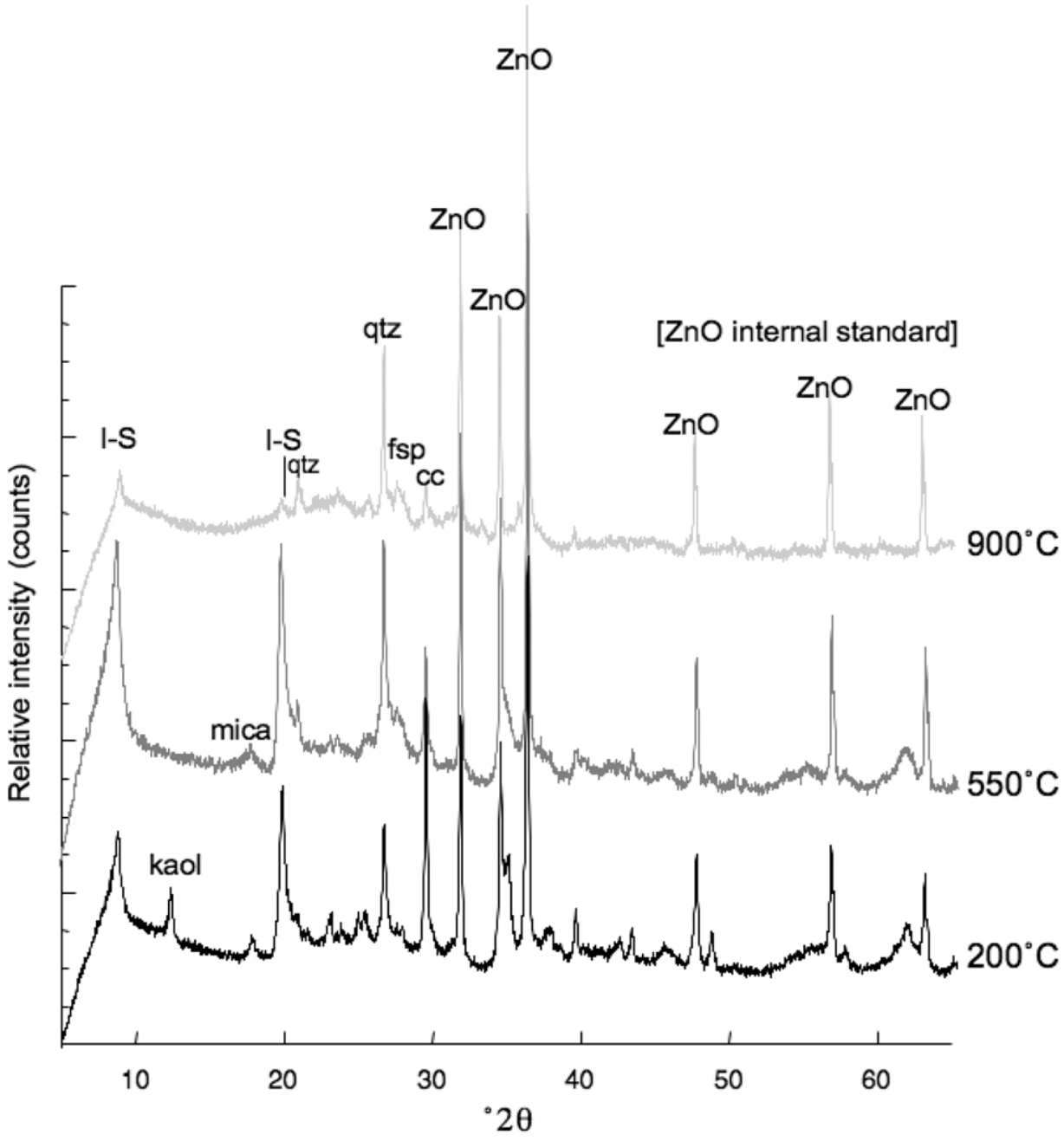

Figure 5.
Random powder XRD patterns (CuKα radiation) of heated CsAg02 clay showing loss of smectite as the clay structure breaks down.

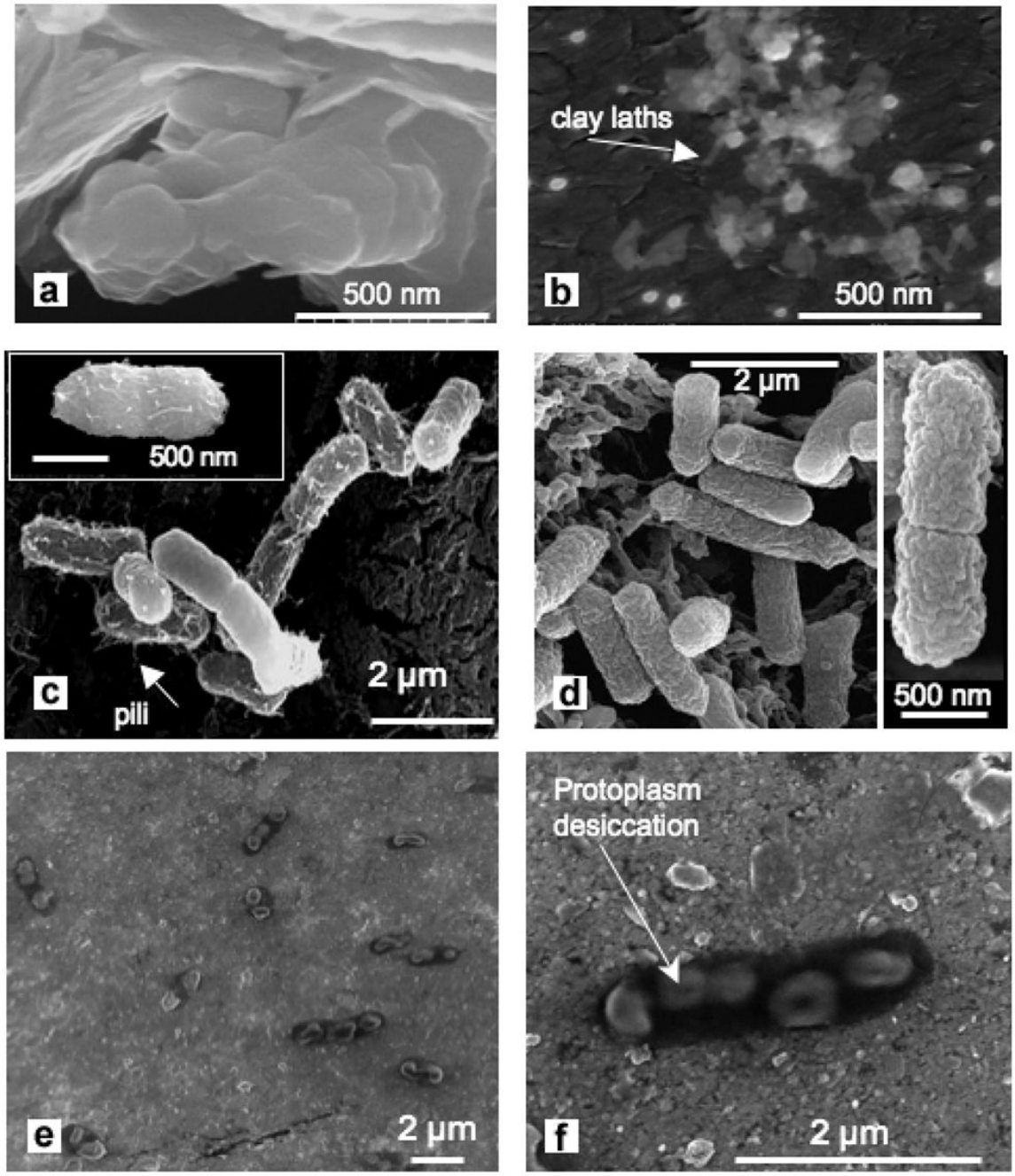

Figure 6.
Field emission SEM photomicrographs showing: (a) 200 nm hexagonal crystals of CsAg02 (Au-coated); (b) 20×100 nm lath-shaped crystals in the same sample (no coat); (c) *E. coli* prepared by critical point drying (CPD), before incubation with clay; (d) *E. coli* incubated with CsAg02 for 6 h, prepared by CPD; (e) *E. coli* incubated with CsAg02 for 6 h imaged with no chemical preparation; (f) close-up of *E. coli* showing no orientation of clay around cell wall or penetration of the bacteria.

Table 1

Bulk mineralogy of the two French green clays determined by XRD and interpreted using *RockJock* full-spectrum matching (Eberl, 2003).

Sample name **Mineral**	**CsAr02** **(wt.%)**	**Mineral**	**CsAg05** **(wt.%)**	**CsAg02** **(wt.%)**	**CsAg02 (<0.2 μm)** **(wt.%)**
NON-CLAYS		NON-CLAYS			
Quartz	18.3	Quartz	1.2	2.7	0.0
Calcite	15.9	Calcite	5.7	3	0.0
Intermediate microcline feldspar	3.0	Intermediate microcline feldspar	2.8	3.9	4.7
Intermediate microcline feldspar	1.4	Orthoclase feldspar	2.6	3.2	0.9
Albite feldspar (Cleavelandite)	0	Albite feldspar (cleavelandite)	1.4	1.8	
Total non-clays	38.6	Total non-clays	13.6	14.6	5.6
CLAYS		CLAYS			
1*Md* illite (+ dioct mica and smectite)	23.1	1*Md* illite (+ dioct mica and smectite)	35.8	24.5	57.9
Ferruginous smectite	14.5	Ferruginous smectite	33.9	32.6	28.9
1*M* Illite (R>2; 88%I)	10.6	1*M* Illite (R >2; 88%I)	10.6	15.6	0.0
Chlorite	4.2	Chlorite			1.6
Mg-chlorite (clinochlore)	1.9	Phlogopite ($2M_1$)	2.8	3.7	0.0
Muscovite ($2M_1$)	6.1				
Total clays	60.3	Total clays	83.1	76.4	88.3
Total	98.9	Total	96.8	91	94.0
Full pattern degree of fit:	0.10	Full pattern degree of fit:	0.09	0.07	0.04

Table 2

Comparison of the major oxides in the two French clays (<2 μm fraction), determined by electron microprobe analysis.

Oxide	CsAr02 (wt.%)	CsAg02 (wt.%)
SiO_2	50.84	59.98
TiO_2	0.00	0.17
Al_2O_3	19.95	18.60
Fe_2O_3*	5.79	6.14
MgO	0.04	4.76
MnO	0.04	0.05
CaO	6.36	1.22
Na_2O	0.12	2.89
K_2O	1.89	3.36
Sum =	85.02	97.17
LOI	3.08	1.92
C	1.68	0.88
S	0.19	0.01
N	0.03	0.02
P	0.15	0.001
Cl	0.01	n.d.

* Total Fe calculated as Fe_2O_3

LOI = loss on ignition

Table 3

Comparison of the ICP-MS results for the two French clays. Analyses were of dissolved clay, exchange solution, and soluble elements (aqueous leachate). Shaded lines denote elements discussed in the text.

	Bactericidal CsAg02					Non-bactericidal CsAr02				
Mass element	Dissolved CsAg02 Clay (ppm)	NH_4-XC CsAg02 (ppm)	NH_4-XC CsAg02 (mM)	Leachate (aq) CsAg02 (ppm)	Leachate (aq) CsAg02 (mM)	Dissolved CsAr02 clay (ppm)	NH_4-XC CsAr02 (ppm)	NH_4-XC CsAr02 (mM)	Leachate (aq) CsAr02 (ppm)	Leachate (aq) CsAr02 (mM)
7 Li	112.0	1.0	1.44E−01	2.8*	4.03E−01	76	1.0	1.44E−01	0.686	9.88E−02
9 Be	4.5	0.001	1.11E−04			2	0.002	2.22E−04	0.0005	5.99E−05
11 B	135	0.5	4.63E−02	9.6	8.88E−01	77.3	0.4	3.70E−02	2.64	2.44E−01
23 Na	18750	108	4.70E+00	3720	1.62E+02	1150	85	3.70E+00	174	7.57E+00
24 Mg	18250	721	2.97E+01	12	5.10E−01	13100	424	1.74E+01	60.4	2.48E+00
27 Al	72000	—	9.27E−02	101	3.74E+00	68000	10.2	3.78E−01	18.86	6.99E−01
28 Si	315	96	3.42E+00	148	5.27E+00	292	134	4.77E+00	86	3.06E+00
31 P	1250	7.2	2.32E−01	8.9*	2.87E−01	640	8.5	2.74E−01	1.16	3.75E−02
39 K	30500	768	1.96E+01	154	3.94E+00	30600	636	1.63E+01	246	6.29E+00
44 Ca	20250	11	2.74E−01	70	1.75E+00	87700	13	3.24E−01	446	1.11E+01
47 Ti	2825	0.108	2.26E−03	0.940*	1.96E−02	3880	0.297	6.20E−03	0.18	3.76E−03
51 V	72.5*	0.029	5.69E−04	0.430	8.44E−03	94	0.042	8.24E−04	0.057	1.12E−03
52 Cr	59	0.032	6.16E−04	0.026	5.00E−04	74	0.059	1.13E−03	0.0095	1.83E−04
55 Mn	723	10	1.82E−01	1.1	2.00E−02	520	11	2.00E−01	0.119	2.17E−03
56 Fe	33375	6.1	1.09E−01	5.6	1.00E−01	35100	5.5	9.85E−02	12.54	2.25E−01
59 Co	10.3	0.040	6.79E−04	0.002	3.39E−05	10.6	0.047	7.98E−04	0.0035	5.91E−05
60 Ni	28.3	0.288	4.91E−03	0.088	1.50E−03	34	0.296	5.04E−03	0.0218	3.71E−04
63 Cu	22.5	0.541	8.51E−03	0.054	8.50E−04	10.1	0.636	1.00E−02	0.0444	6.99E−04
66 Zn	100	0.216	3.30E−03	0.100	1.53E−03	71	0.255	3.90E−03	0.086	1.32E−03
69 Ga	21.5	0.001	1.58E−05	0.0028*	1.30E−02	16.1	0.0034	4.88E−05	0.0176	2.52E−04
72 Ge	1.25*	0.001	6.89E−06			1.9	0.0005	6.89E−06	0.0004	5.51E−06
75 As	52.5*	0.02	2.67E−04	5.2*	6.94E−02	3.53	0.02	2.67E−04	0.0182	2.43E−04
77 Se	1.25*	0.108	1.37E−03	0.03*	3.80E−04	0.2	0.085	1.08E−03	0.12	1.52E−03
85 Rb	118	3.240	3.79E−02	0.360	4.21E−03	114	2.97	3.47E−02	0.1286	1.50E−03
88 Sr	340	154	1.76E+00	1.2	1.32E−02	230	255	2.91E+00	10.4	1.19E−01
89 Y	12.3	0.003	3.37E−05	0.006	6.75E−05	18.8	0.006	6.75E−05	0.0112	1.26E−04
90 Zr	51.8	0.018	1.97E−04			101	0.025	2.74E−04	0.019	2.08E−04
93 Nb	12*	—	—	—	—	14.3	—	—	0.0004	4.74E−06
95 Mo	0.8	0.040	4.17E−04	0.156	1.63E−03	0.36	0.04	4.17E−04	0.013	1.36E−04
109 Ag	0.5	—	—	0.0048*	4.45E−05	0.331	—	—	0.0001	9.27E−07
111 Cd	0.3	0.0100	8.90E−05			0.21	0.01	8.90E−05	0.0003	2.49E−06
118 Sn	6.0	0.0004	3.48E−06	0.0024	2.09E−05	2.47	0.0004	3.48E−06	0.0006	5.57E−06
123 Sb	1.8	0.006	4.93E−05	0.070	5.75E−04	0.563	0.005	4.11E−05	0.0078	6.37E−05
133 Cs	14.8	0.072	5.42E−04	0.002	1.50E−05	8.1	0.072	5.42E−04	0.0008	5.72E−06
138 Ba	418	144.0	1.05E+00	0.620	4.51E−03	393	119	8.67E−01	2.134	1.55E−02
139 La	21.0	0.0043	3.10E−05	0.016*	1.15E−04	35.5	0.0051	3.67E−05	0.0106	7.63E−05
140 Ce	45.5	0.0040	2.85E−05			69.4	0.0072	5.14E−05	0.034	2.43E−04
141 Pr	5.8	0.0005	3.55E−06	0.0024	1.70E−05	7.76	0.0008	5.68E−06	0.0036	2.54E−05
146 Nd	19.8	0.0030	2.08E−05	0.0076	5.27E−05	28.2	0.005	3.47E−05	0.0152	1.05E−04
147 Sm	4.0	0.0011	7.32E−06	0.0012	7.98E−06	5.5	0.0013	8.65E−06	0.0033	2.22E−05
153 Eu	1.0	0.0029	1.91E−05			1.31	0.0025	1.65E−05	0.0016	1.05E−05
157 Gd	3.8	0.0014	8.90E−06	0.0016	1.02E−05	5.5	0.0017	1.08E−05	0.0035	2.23E−05
159 Tb	0.5	—	—	—	—	0.79	0.0001	6.29E−07	0.0005	3.15E−06
163 Dy	2.8	0.0002	1.23E−06	0.0008	4.92E−06	4.1	0.0004	2.46E−06	0.0024	1.46E−05
165 Ho	0.5	—	—	—	—	0.82	0.0003	1.82E−06	0.005	3.03E−05
166 Er	1.75	0.0001	5.98E−07	—	—	2.52	0.0002	1.20E−06	0.0012	7.05E−06
169 Tm	0.3	0.0001	5.92E−07	—	—	0.356	0.0001	5.92E−07	0.0001	8.29E−07
172 Yb	1.5	0.0001	5.78E−07	—	—	2.5	0.0003	1.73E−06	0.0008	4.85E−06
178 Hf	1.5	0.0006	3.36E−06	—	—	3.9	0.0006	3.36E−06	0.0002	1.34E−06
181 Ta	1.8	—	—	—	—	2.47	—	—	0.0001	3.32E−07

Mass element	Bactericidal CsAg02 Dissolved CsAg02 Clay (ppm)	Bactericidal CsAg02 NH_4-XC CsAg02 (ppm)	Bactericidal CsAg02 NH_4-XC CsAg02 (mM)	Bactericidal CsAg02 Leachate (aq) CsAg02 (ppm)	Bactericidal CsAg02 Leachate (aq) CsAg02 (mM)	Non-bactericidal CsAr02 Dissolved CsAr02 clay (ppm)	Non-bactericidal CsAr02 NH_4-XC CsAr02 (ppm)	Non-bactericidal CsAr02 NH_4-XC CsAr02 (mM)	Non-bactericidal CsAr02 Leachate (aq) CsAr02 (ppm)	Non-bactericidal CsAr02 Leachate (aq) CsAr02 (mM)
182 W	2.8	0.0050	2.72E−05	0.0004	2.18E−06	1.95	0.005	2.72E−05	0.0005	2.94E−06
185 Re	—	0.022	1.18E−04	—	—	0	0.013	6.98E−05	0.011	5.91E−05
197 Au	1.3	—	—	—	—	0.124	0.0001	5.08E−07	—	—
205 Tl	1.0	0.0320	1.57E−04			0.58	0.038	1.86E−04	0.0002	9.7857E−07
208 Pb	34.0	0.0046	2.22E−05	0.0052	2.51E−05	14.1	0.0051	2.46E−05	0.0085	4.0927E−05
209 Bi	1.0	0.0001	4.79E−07			0.16	0.0001	4.79E−07	0.0001	3.8281E−07
232 Th	13.3	0.0022	9.48E−06	0.0040	1.72E−05	12.6	0.0042	1.81E−05	0.0033	1.4049E−05
238 U	7.3	0.2200	9.24E−04	0.9800	4.12E−03	2.45	0.21	8.82E−04	0.0182	7.6461E−05
pH	10.23					7.64				

Relative standard deviation ≤5% except where noted by *

–: not detected

Clays Clay Miner. Author manuscript; available in PMC 2008 December 10.

Table 4

ICP-MS analysis of elements in the dissolved antibacterial clay (CsAg02). Results are reported in ppm normalized to weight of clay. Elements discussed are shaded.

CsAg02 Mass element	Bulk (ppm)	1.032.0 μm (ppm)	0.231.0 μm (ppm)	<0.2 μm (ppm)
7 Li	112	117	112	157
9 Be	5	6	6	7
11 B	135	150	152	235
23 Na	18750	6075	4225	10800
24 Mg	18250	17100	19000	13750
27 Al	72000	88000	84250	51500
28 Si	315	318	286	403
31 P	1250	1250	1500	2088
39 K	30500	48750	37500	24000
44 Ca	20250	16000	11225	8200
47 Ti	2825	6600	3823	2375
51 V	73*	114	94	104
52 Cr	59	90	76	81
55 Mn	723	578	407	405
56 Fe	33375	40000	39750	44750
59 Co	10	13	10	11
60 Ni	28	32	27	34
63 Cu	23	33	24	31
66 Zn	100	140	135	160
69 Ga	22	33	29	31
72 Ge	1.3*	2.0*	2	1.8*
75 As	53*	48*	32	43
77 Se	1.3*	0.8*	1	1.0*
85 Rb	118	198	205	53
88 Sr	340	308	250	198
89 Y	12	14	15	14
90 Zr	52	83	48	54
93 Nb	12	30	16	12
95 Mo	0.8	1.8	1.5	0.8
109 Ag	0.5	7.3	1.3	1.3
111 Cd	0.3	0.3	0.2	0.2
118 Sn	6	11	9	8
123 Sb	2	2	2	2
133 Cs	15	24	23	13
138 Ba	418	618	378	100
139 La	21	31	30	16
140 Ce	46	63	58	43
141 Pr	6	8	8	5
146 Nd	20	27	25	19
147 Sm	4.0	5.3	4.8	4.0
153 Eu	1.0	1.3	1.0	0.8
157 Gd	3.8	5.0	4.8	4.0
159 Tb	0.5	0.8	0.8	0.8
163 Dy	2.8	3.5	3.3	3.3
165 Ho	0.5	0.8	0.5	0.5
166 Er	1.8	2.0	1.8	1.8
169 Tm	0.3	0.3	0.3	0.3
172 Yb	1.5	2.0	1.5	1.5
178 Hf	1.5	2.5	1.5	2.0
181 Ta	1.8	3.8	2.5	2.5
182 W	2.8	7.5	3.5	3.3
197 Au	1.3	1.3	1.3	1.3
205 Tl	1.0	2.0	1.5	1.3
208 Pb	34	55	34	33
209 Bi	1.0	1.5	1.0	1.3
232 Th	13	14	14	14
238 U	7	8	7	9

Relative standard deviation ≤5% except where noted by *

Table 5

Contact-angle measurements for water, glycerol, and diiodomethane on oriented <0.2 μm clay films. The surface tension values for these liquids are listed in van Oss (1994). The contact angles have a standard deviation of approximately 2°. Solution of the simultaneous Young-Dupré equations yields the surface tension values (as mJ/m^2) in the lower part of the table (+: electron acceptor; −: electron donor; Giese and van Oss, 2002)

	CsArO2	CsAgO2
Water	2	10
Glycerol	22	7
Diiodomethane	30	34
γ^{LW}	42.5	44.2
γ^{+}	2.8	1.4
γ^{-}	43.7	50.4